



저작자표시-비영리-변경금지 2.0 대한민국

이용자는 아래의 조건을 따르는 경우에 한하여 자유롭게

- 이 저작물을 복제, 배포, 전송, 전시, 공연 및 방송할 수 있습니다.

다음과 같은 조건을 따라야 합니다:



저작자표시. 귀하는 원저작자를 표시하여야 합니다.



비영리. 귀하는 이 저작물을 영리 목적으로 이용할 수 없습니다.



변경금지. 귀하는 이 저작물을 개작, 변형 또는 가공할 수 없습니다.

- 귀하는, 이 저작물의 재이용이나 배포의 경우, 이 저작물에 적용된 이용허락조건을 명확하게 나타내어야 합니다.
- 저작권자로부터 별도의 허가를 받으면 이러한 조건들은 적용되지 않습니다.

저작권법에 따른 이용자의 권리는 위의 내용에 의하여 영향을 받지 않습니다.

이것은 [이용허락규약\(Legal Code\)](#)을 이해하기 쉽게 요약한 것입니다.

[Disclaimer](#)

석사학위논문

Anti-cancer Effect of Fenbendazole
Incorporated PLGA Nanoparticles
in Ovarian Cancer

계명대학교 대학원
의학과

최준국

지도교수 권상훈

2022년 8월

Anti-cancer Effect of Fenbendazole Incorporated PLGA Nanoparticles in Ovarian Cancer

지도교수 권 상 훈

이 논문을 석사학위 논문으로 제출함

2 0 2 2 년 8 월

계 명 대 학 교 대 학 원

의학과 산부인과학 전공

최 준 국

최준국의 석사학위 논문을 인준함

주 심 조 치 흙

부 심 권 상 훈

부 심 신 소 진

계 명 대 학 교 대 학 원

2 0 2 2 년 8 월

감사의 말씀

본 논문을 제출하기까지 아낌없이 보살펴 주신 권상훈 지도교수님께 진심으로 감사드리며 석사 학위를 준비하기 위한 기간이 오래 되었음에도 기다려주심에 다시 한번 감사의 말씀을 드립니다. 더불어 바쁘신 가운데에도 많은 관심과 조언해 주신 조치흠 교수님과 신소진 교수님께도 감사의 말씀을 드립니다.

비록 의국을 떠나있는 몸이지만 항상 저의 뿌리는 동산병원 산부인과에 있음을 기억하고 있으며, 산부인과 의사로 살아가는데 기본을 가르쳐 주신 스승님들께 항상 감사하는 마음으로 살아가겠습니다.

2022년 8월

최 준 국

Table of Contents

1. Introduction	1
2. Materials and Methods	3
3. Results	8
4. Discussion	20
5. Summary	23
References	24
Abstract	30
국문초록	31

List of Figures

- Figure 1. MTT assay to cell viability by natural form of fenbendazole in epithelial ovarian cancer cell line 12
- Figure 2. The efficacy of oral natural fenbendazole on tumor growth and on body weight change using cell-line xenograft mouse model for epithelial ovarian cancer 13
- Figure 3. Physical properties and cell viability analysis of PLGA-NPs and FZ-PLGA-NPs 15
- Figure 4. FACS analysis in epithelial ovarian cancer cells using PLGA-NPs and compared with FZ-PLGA-NPs containing 1 μ M of fenbendazole 17
- Figure 5. Anti-cancer effect of FZ-PLGA-NPs in vitro and in vivo models 18
- Figure 6. Western blot analysis to evaluate the cell signaling pathway in epithelial ovarian cancer cells 19

List of Supplementary Figures

Supplementary Figure 1. Aggregated fenbendazole in the intraperitoneal cavity of mice	14
--	----

1. Introduction

Epithelial ovarian cancer (EOC) is the second most common and leading cause of mortality among all gynecologic malignancy (1). In addition to the standard treatment of primary cytoreductive surgery followed by platinum-based combination chemotherapy, recent advances in treatment modality of including bevacizumab and poly-ADP-ribose polymerase (PARP) inhibitors are being widely used in therapeutic and maintenance settings (2,3). Despite a good response to primary treatment, most patients with advanced disease experience relapse and eventually die from the disease (4). Patients with advanced EOC have a five-year survival of only 40% (5), and there are an unmet needs to find new therapeutic drugs for EOC.

Drug repurposing has become a promising option for finding new anti-cancer drugs at lower cost and in a shorter time. Fenbendazole (FZ), a widely used benzimidazole anthelmintics drug for treatment of gastrointestinal parasites, has recently been shown to have anti-cancer effects against several cancer types (6-9). Furthermore, it has been reported that benzimidazole anthelmintics exhibit anti-cancer effects in paclitaxel and doxorubicin-resistant cancer cells (10,11). The suggested mechanisms of its antitumor effects are disruption of microtubule polymerization, G2/M phase cell cycle arrest, and anti-angiogenesis (12). Especially in ovarian cancer models, potential anti-vascular endothelial growth factor (VEGF) activity of benzimidazole analogues has been reported, showing inhibition of peritoneal tumor growth and ascites formation through intraperitoneal (IP) administration (13-15).

However, FZ and its analogues have low water solubility and poor

bioavailability (16), which is a major obstacle to the clinical application as an anti-cancer agent. Drug delivery with nanoparticles has been recently proposed to overcome some of the challenges of drug delivery, such as low solubility and permeability of drugs (17). Several nanoparticle platforms have been developed to enhance drug delivery (18-20). Poly (d,l-lactide-co-glycolide) acid (PLGA) polymer is a suitable option for clinical and biological application owing to its low toxicity, biocompatibility, biodegradability, and low immunogenicity (21). Taking this into consideration, we utilized PLGA as the polymer matrix and developed a method of encapsulating FZ in PLGA-nanoparticle to increase the hydrophilicity of FZ.

In this study, we aimed to investigate the anti-cancer effect of FZ on EOC models including in vitro and in vivo experiments. We also aimed to explore the anti-cancer effect of FZ with different drug delivery modes on EOC using natural FZ and FZ-encapsulated PLGA-nanoparticle (FZ-PLGA-NP).

2. Materials and Methods

2.1. Cell lines and treatments:

Human EOC cell lines (HeyA8, SKOV3ip1, A2780-CP20, HeyA8-MDR and SKOV3-TR) were a gift from Dr. Anil K. Sood, Department of Cancer Biology, University of Texas M.D. Anderson Cancer Center, TX, USA. The A2780 was purchased from the European Collection of Cell Cultures (ECACC, Cat No.93112520). All of ovarian cancer cells were maintained in Roswell Park Memorial Institute (RPMI) 1640 supplemented with 10% fetal bovine serum (FBS), and all cells were maintained in humidified incubator (37 °C, 5% CO₂). FZ, Poly (d,l-lactide-co-glycolide) acid (PLGA, Resomer RG502H, monomer ratio 50:50, Mw 7-17 kDa), and Poly (vinyl alcohol) (PVA, 80% hydrolyzed, Mw 9-10 kDa) were purchased from Sigma-Aldrich (St. Louis, MO, USA). FZ was re-suspended in dimethyl sulfoxide (DMSO) at a concentration of 5 mg/mL.

2.2. Preparation of FZ-PLGA-NPs:

We prepared FZ-PLGA-NPs by an oil-in water (o/w) emulsion method (22). Briefly, 20 mg of FZ was dissolved in 2 mL DMSO and mixed with 2 mL chloroform containing 80 mg of PLGA as an oil phase. The oil phase was mixed with 10 mL of 2.0% PVA solution using a probe-type sonicator (SONICS, USA) at 4 °C for 10 min (40 pulses of 5 s with 3 s gap). Chloroform and DMSO in the emulsion were evaporated using rotary evaporator at 30 °C under a vacuum. After evaporation, FZ-PLGA-NPs were washed thrice by centrifugation at 13,000 rpm for 20

min and stored at 4 °C until use.

The size and zeta potential of the FZ-PLGA-NPs were measured by dynamic light scattering using an electrophoretic light scattering photometer (SZ-100, Horiba, Kyoto, Japan) (23). The loading efficiency of FZ in the FZ-PLGA-NPs was measured by UV-vis spectrophotometer (UV-mini, Shimadzu, Japan) at wavelength of 285 nm (24).

2.3. Cell proliferation assay:

Cells were plated in culture medium in a 96-well plate at 3×10^3 cells/well. After 24 hours, cells were treated with FZ or FZ-PLGA-NPs and the assay was performed at 24, 48 and 72 hours. For proliferation assays, cells were stained with 3-(4,5-Dimethylthiazol-2-yl)-2,5-diphenyltetrazolium bromide (MTT; Amresco, Solon, OH, USA), after 4 hr of additional incubation, the medium was discarded, 100 μ L of acidic isopropanol (0.1 N HCL in absolute sopropanol) was added, and the plate was shaken gently. Absorbance was measured on an enzyme linked immunosorbent assay (ELISA) reader at a test wavelength of 540 nm.

2.4. Apoptosis assay:

Cell apoptosis was measured at 48 hours using the Annexin V-FITC apoptosis Detection Kit-1 (BD Pharmingen, San Diego, CA, USA) according to the manufacturer's protocol. Briefly, cells were washed twice in phosphate buffered saline (PBS) and the pellet was re-suspended in annexin V binding buffer at a concentration of 10^6 cells/mL. Annexin V FITC and propidium iodide (PI) were added (5 μ l

to each per 10^5 cells). Samples were gently mixed and incubated for 15 minutes at room temperature in the dark before the fluorescence activated cell sorter (FACS) analysis.

2.5. Western blot analysis:

Cells were lysed in a PRO-PRE Protein Extraction Solution (Intron Biotechnology, Seongnam, Korea). Protein concentration was decided using a Bradford assay kit (Bio-Rad, Hercules, CA, USA). Cells (40 μ g of total protein) were separated on 7.5% or 10% acrylamide gels by sodium dodecyl sulfate-polyacrylamide gel electrophoresis (SDS-PAGE) and transferred to Immobilon-P transfer membrane (Merck Millipore, Burlington, MA, USA).

Membranes were blocked for 1 hour with 5% skim milk in Tris-buffered saline containing 0.1% Tween-20 at room temperature. Protein bands were probed with total-PI3K and phospho-PI3K (p-PI3K), total-AKT and phospho-AKT (p-AKT), total-mTOR and phospho-mTOR (p-mTOR) total-ERK and phospho-ERK (p-ERK) (Cell Signaling Technology, Danvers, MA, USA) antibodies at 1:1000 dilutions or with total-S6K1 and phospho-S6K1 (p-S6K1), β -actin (Santa Cruz Biotechnology, Dallas, TX, USA) antibodies at a 1:2000 dilution and then tagged with horseradish peroxidase-conjugated anti-rabbit antibody (GE Healthcare, Piscataway, NJ, USA). Bands were envisioned by enhanced chemiluminescence using an ECL kit (Amersham Biosciences) according to the manufacturer's protocol.

2.6. Immunohistochemistry:

Immunohistochemical studies were performed on formalin-fixed, paraffin-embedded, 4- μ m-thick tissue sections. Immunostaining for Ki-67 (NB600-1252; NOVUS Biologicals, Centennial, CO, USA) was performed with a BOND-MAX™ automated immunostaining device (Leica Biosystems, Melbourne, Australia) and the Bond™ Polymer purification detection kit (Vision Biosystems, Melbourne, Australia). Briefly, antigen retrieval was carried out in ER1 buffer at 97 °C for 20 minutes. The endogenous peroxidase activity was blocked with 3% hydrogen peroxidase for 10 minutes, and the antibody was diluted at room temperature at 1:200 for 15 minutes. Apoptotic-positive cells were analyzed by TUNEL assay using the ApopTag Peroxidase In Situ Apoptosis Detection Kit (Merck Millipore, Burlington, MA, USA) as described above.

2.7. Animal care and orthotopic implantation of tumor cells:

Female BALB/c nude mice were purchased from Orient Bio, Seongnam, Korea. This study was reviewed and approved by the Institutional Animal Care and Use Committee (IACUC) of the Samsung Biomedical Research Institute (protocol No. H-A9-003), which is accredited by the Association for the Assessment and Accreditation of Laboratory Animal Care International (AAALAC International) and abides by the guidelines of the Institute of Laboratory Animal Resources (ILAR).

The mice used in these experiments were 6 to 8 weeks old. To establish orthotopic models, HeyA8 (2.5×10^5 cells/0.2 mL HBSS) and HeyA8-MDR (1×10^6 cells/0.2 mL HBSS) were injected into the

peritoneal cavity of mice. For the patient-derived xenograft (PDX) model of EOC, a specimen of the patient's tumor collected in the operating room was cut to less than 2-3 mm and transplanted into the subrenal capsule of the left kidney of a mouse by continuous transplantation. We selected a PDX from a 53-year-old woman with FIGO stage IIIC and high-grade serous histology ovarian cancer. She was treated with primary cytoreductive surgery followed by six cycles of paclitaxel-carboplatin combination chemotherapy. There was no residual tumor after primary surgery, and her progression-free survival was 45 months.

FZ was orally or intravenously administered (3 times/week). Mice (n = 10 per group) were monitored daily for tumor development and were sacrificed on day 21-28 after injection of cancer cells, on day 70-85 (PDX model), or when considered moribund. Total body weight and tumor weight were recorded at the time of sacrifice. Tumors were fixed in formalin and embedded in paraffin or snap frozen in OCT compound (Sakura Finetek Japan, Tokyo, Japan) in liquid nitrogen.

2.8. Data analysis:

The Mann-Whitney U test was used to evaluate significance and to compare differences among groups for both in vitro and in vivo assays using a statistical software package (Prism; GraphPad, San Diego, CA, USA). P values less than 0.05 were considered statistically significant.

3. Results

3.1. Effect of natural FZ on cell viability in EOC cells:

We first confirmed the *in vitro* anti-cancer effect of FZ in EOC cell lines. We performed MTT assay to investigate whether natural form of FZ inhibits with cell proliferation of EOC (Figure 1). The results showed that treatment with FZ significantly decreased cell viability of chemosensitive (A2780, HeyA8, SKOV3ip1) EOC cells in a dose-dependent manner at 24 hours. In chemoresistant EOC cells, FZ significantly reduced cell viability in A2780-CP20 and HeyA8-MDR, but not in SKOV3-TR. When we extended exposure time of the FZ to 48 hours, significant reduction in cell proliferation was observed with treatment of FZ in all six EOC cell lines. Similar results were observed when exposure time was extended to 72 hours. The half-maximal inhibitory concentration (IC₅₀) values determined ranged from 0.34 μ M to 0.85 μ M for natural FZ, with SKOV3-TR cell line exhibiting the least sensitivity.

3.2. *In vivo* efficacy of natural FZ in xenograft mouse models for EOC:

We next investigated the efficacy of FZ on tumor growth *in vivo* using cell-line xenograft mouse model for EOC. HeyA8 and HeyA8-MDR cells were implanted into the peritoneal cavity of female nude mice. The mice treated with 1 mg dose of natural FZ did not show reduction of tumor weight in both HeyA8 and HeyA8-MDR models (Figure 2A).

Likewise, no tumor reduction was observed when the dose of FZ was increased to 10 mg (Figure 2B).

Since FZ has low systemic bioavailability due to extensive first-pass metabolism when administered orally (25), the drug administration route was changed to IP injection. However, it was observed that FZ was aggregated in the intraperitoneal cavity of mice and not absorbed at all (Supplementary Figure 1). Based on these results, we concluded that FZ in natural form could not be delivered to the tumor cells in vivo due to its low water solubility.

3.3. Characteristics of FZ-PLGA-NPs and effect on cell viability and apoptosis:

We utilized PLGA as the polymer matrix, and prepared FZ-PLGA-NPs encapsulating FZ to enhance water solubility and absorption of FZ. We first determined physical properties of FZ-PLGA-NPs (Figure 3). The mean particle size and zeta potential were 531 ± 5.31 nm and -30.6 ± 1.36 mV, respectively (Figure 3A&3B). FZ-PLGA-NP has increased particle size due to FZ encapsulation. Representative histogram of the PLGA-NPs and FZ-PLGA-NPs was shown in Figure 3C, which indicate size distributions of NPs. Loading efficiency of FZ in FZ-PLGA-NPs was 89% (Figure 3D).

Next, we assessed the cytotoxic effect of FZ-PLGA-NP and compared with PLGA-NPs without encapsulation of FZ. PLGA-NPs as a control did not show any cytotoxic effect in the tumor cells in all six EOC cell lines. On the other hand, treatment with FZ-PLGA-NP significantly decreased cell viability of chemosensitive and chemoresistant EOC cells (Figure 3E), similar with the results of MTT assay with natural

FZ. The IC₅₀ values determined ranged from 0.12 μ M to 0.81 μ M for FZ-PLGA-NPs, with SKOV3ip1 and SKOV3-TR cell lines exhibiting the least sensitivity. SKOV3ip1 cell line treated with FZ-PLGA-NPs did not reach 50% viability relative to the control. The EOC cell lines that showed the best sensitivity were HeyA8 and HeyA8-MDR.

FACS analysis was performed in EOC cells using FZ-PLGA-NPs containing 1 μ M of FZ to assess apoptosis. Apoptotic cells were measured by Annexin V-incorporation after treatment with FZ-PLGA-NPs, and the results were similar to those from the cell proliferation assay. The apoptotic cells significantly increased after treating A2780, A2780-CP20, HeyA8, HeyA8-MDR, SKOV3ip1, and SKOV3-TR cells with FZ-PLGA-NPs after 48 hours (Figure 4).

3.4. In vivo efficacy of FZ-PLGA-NPs in xenograft mouse models including PDX:

To confirm the anti-cancer effect of FZ-PLGA-NPs of in vitro results, we performed in vivo experiments using EOC cell-line xenografts and PDX models. FZ-PLGA-NPs were administered to the mice intravenously as the formula was hydrophilic. In both HeyA8 and HeyA8-MDR models, treatment with FZ-PLGA-NPs resulted in a significant inhibition of tumor growth compared with the control using PLGA-NPs (Figure 5A). When applied to the PDX model, tumor weight and size after treatment with FZ-PLGA-NPs were significantly reduced compared to the control (Figure 5B). Using harvested tumor tissues, we also confirmed the inhibitory effects of this treatment; the expression of Ki-67, a cell proliferation marker, was significantly decreased after treatment, whereas in TUNEL, a marker of cell death, was

significantly increased. The consistent results were observed in mouse EOC cell line models using HeyA8 and HeyA8-MDR, as well as in the PDX model.

3.5. Mechanism of anti-cancer effect of FZ in EOC cells:

To confirm the reduction in cell proliferation and increase in apoptosis, we evaluated the cell signaling pathway in EOC cells by western blot analysis (Figure 6). Following treatment with FZ-PLGA-NPs in HeyA8 and HeyA8-MDR cells, the expression of p-PI3K and p-AKT, which are the signaling proteins for cell growth and proliferation, were decreased compared to the control and PLGA-NPs-treated cells. Reduction in phosphorylated form of mTOR, ERK, and S6K1 proteins were also observed with treatment of FZ-PLGA-NPs. These changes of protein expression were not observed when only carrier polymer PLGA-NP was administered. These results suggest that FZ affects cell proliferation through inhibition of PI3K/AKT and mitogen-activated protein kinase (MAPK) signaling pathways.

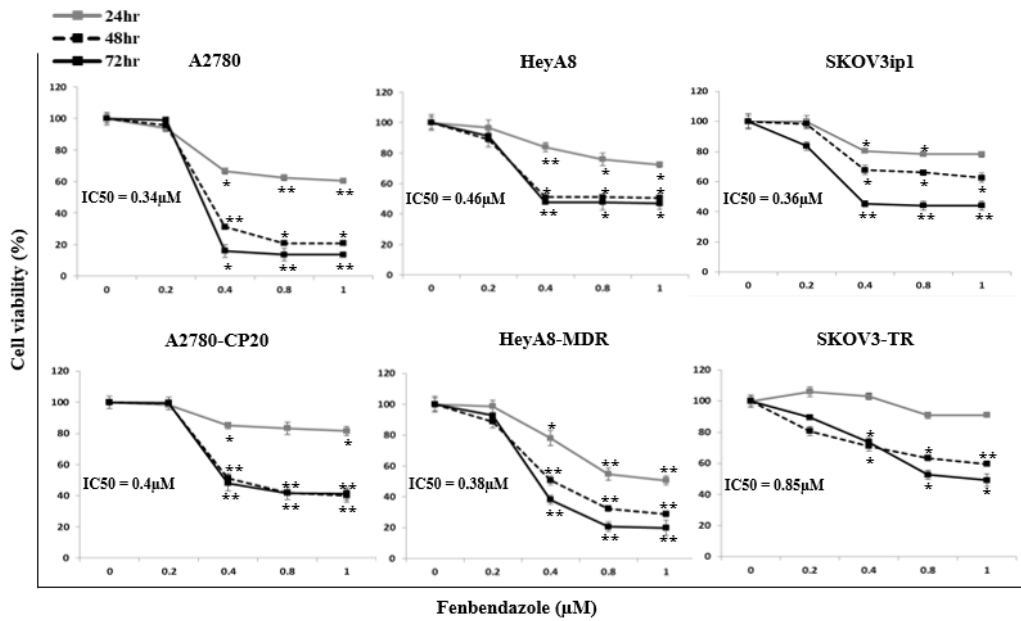
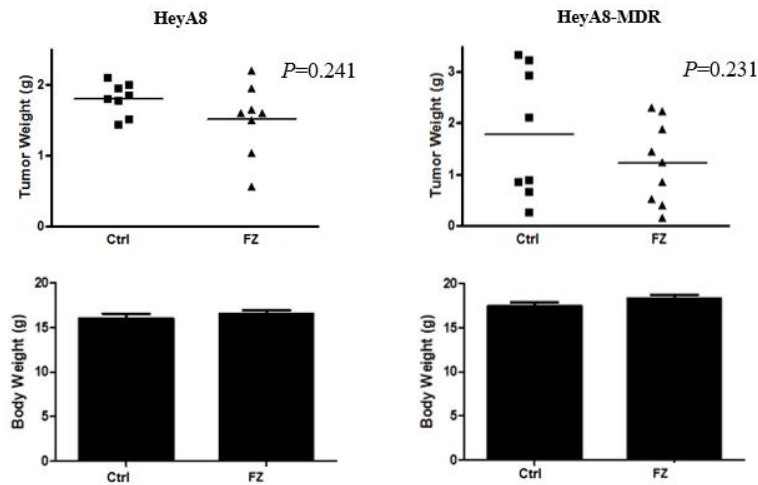


Figure 1. MTT assay to cell viability by natural form of fenbendazole in epithelial ovarian cancer cell line. *: $P < 0.05$; **: $P < 0.001$.

A

Oral dosing of FZ (1mg/mouse)



B

Oral dosing of FZ (10mg/mouse)

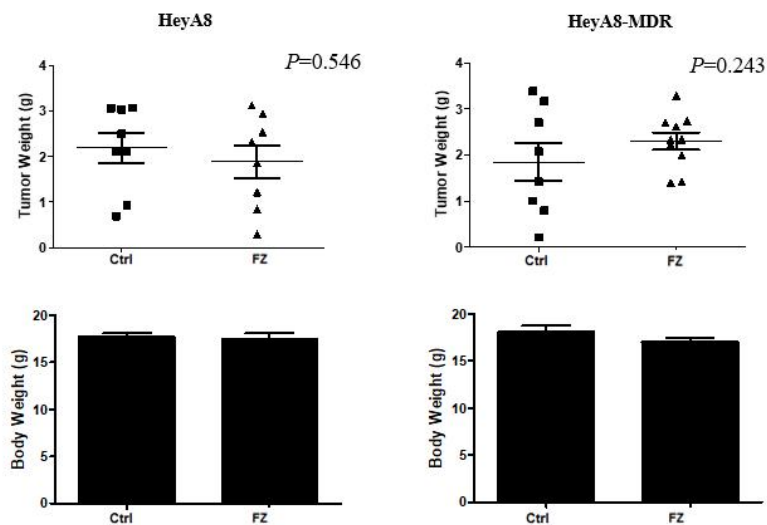
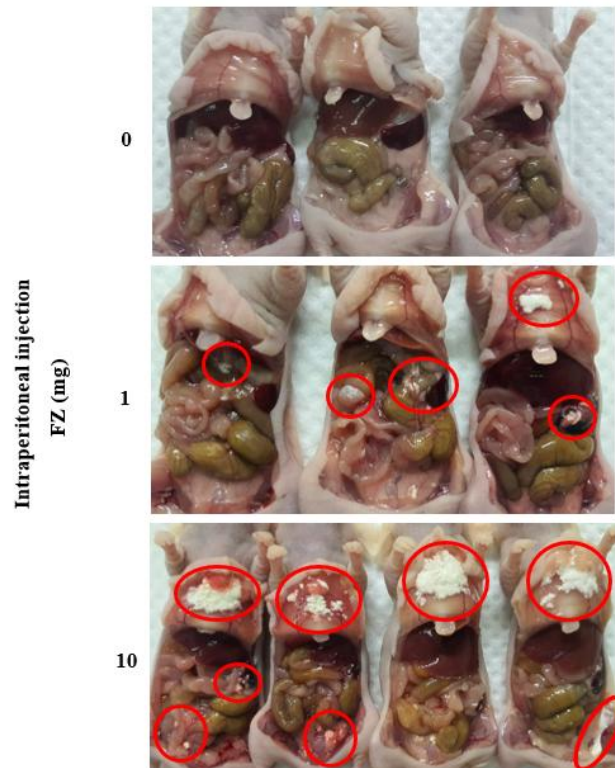
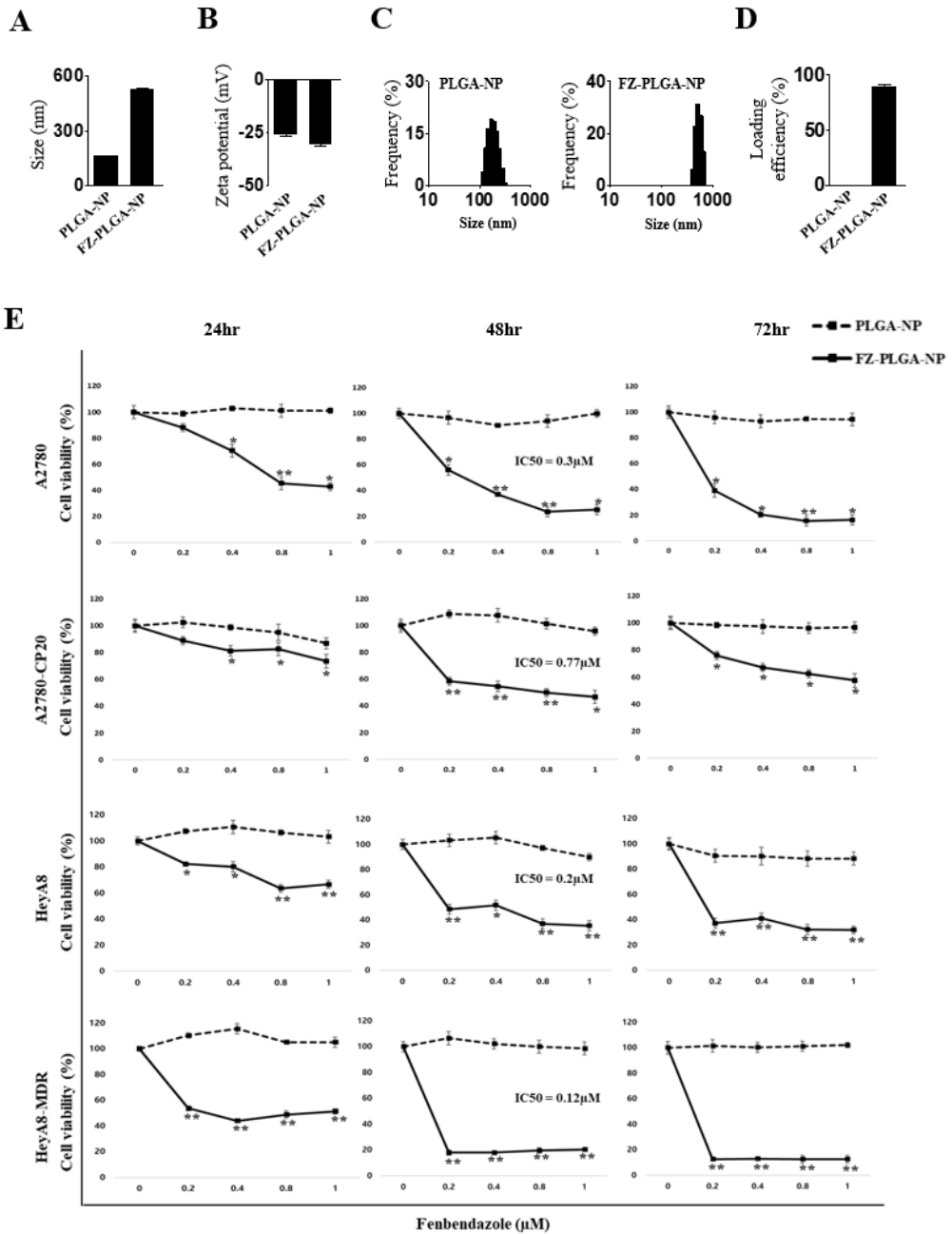


Figure 2. The efficacy of oral natural FZ on tumor growth and on body weight change using cell-line xenograft mouse model for EOC. (A) 1 mg oral dosing of FZ. (B) 10 mg oral dosing of FZ. FZ: fenbendazole; EOC: epithelial ovarian cancer.



Supplementary Figure 1. Aggregated fenbendazole in the intraperitoneal cavity of mice.



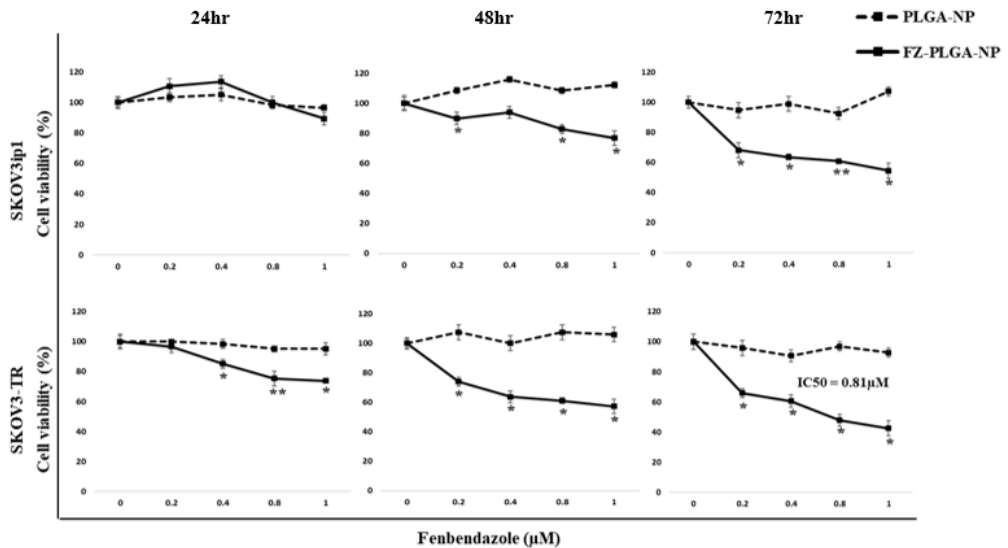


Figure 3. Physical properties and cell viability analysis of PLGA-NPs and FZ-PLGA-NPs. (A) The mean particle size. (B) Zeta potential. (C) Histogram of the PLGA-NPs and FZ-PLGA-NPs. (D) Loading efficiency of FZ in FZ-PLGA-NPs. (E) Cell viability according to FZ-PLGA-NPs and PLGA-NPs of chemosensitive and chemoresistant EOC cells line. *: $P < 0.05$; **: $P < 0.001$. FZ-PLGA-NPs: Fenbendazole-Poly (d,l-lactide-co-glycolide) acid-Nanoparticles; PLGA-NPs: Poly (d,l-lactide-co-glycolide) acid-Nanoparticles; EOC: epithelial ovarian cancer.

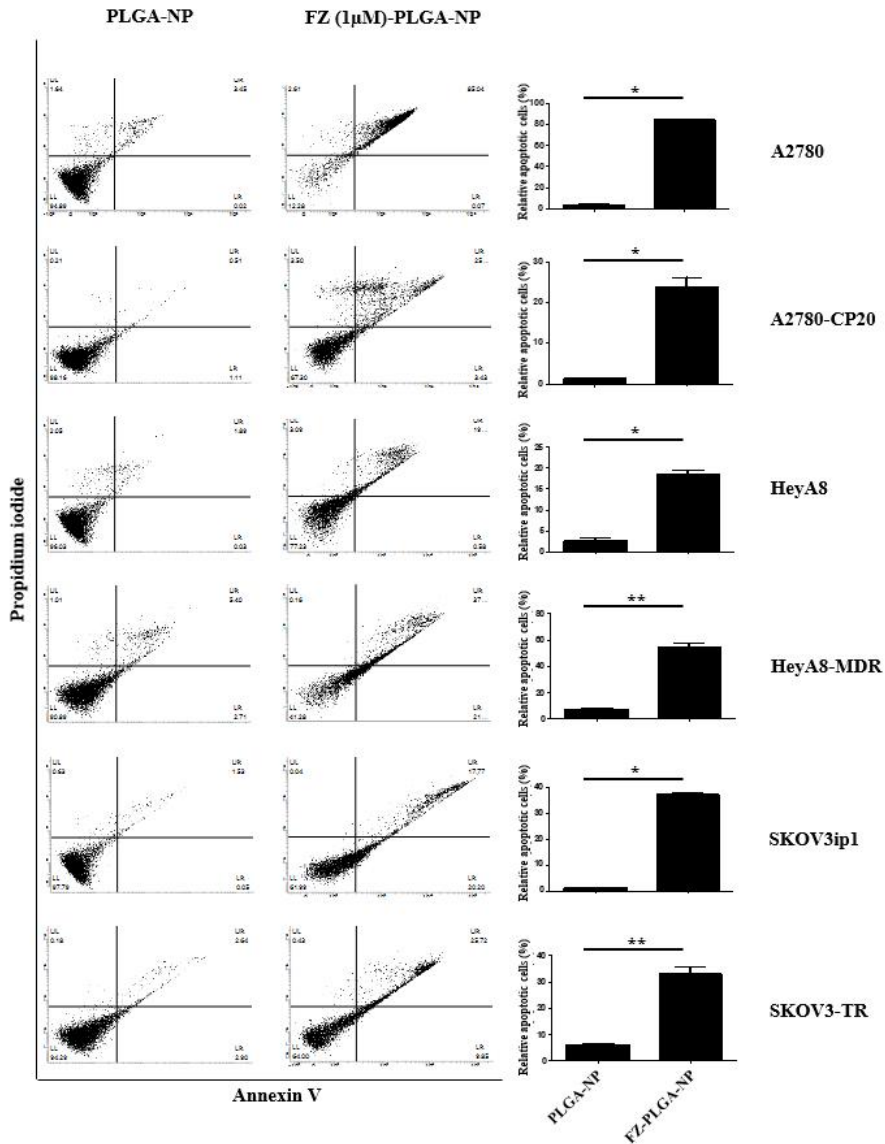


Figure 4. FACS analysis in EOC cells using PLGA-NPs and compared with FZ-PLGA-NPs containing 1 μ M of fenbendazole. *: P < 0.05; **: P < 0.001. EOC: epithelial ovarian cancer; PLGA-NPs: Poly (d,l-lactide-co-glycolide) acid-Nanoparticles; FZ-PLGA-NPs: Fenbendazole-Poly (d,l-lactide-co-glycolide) acid-Nanoparticles.

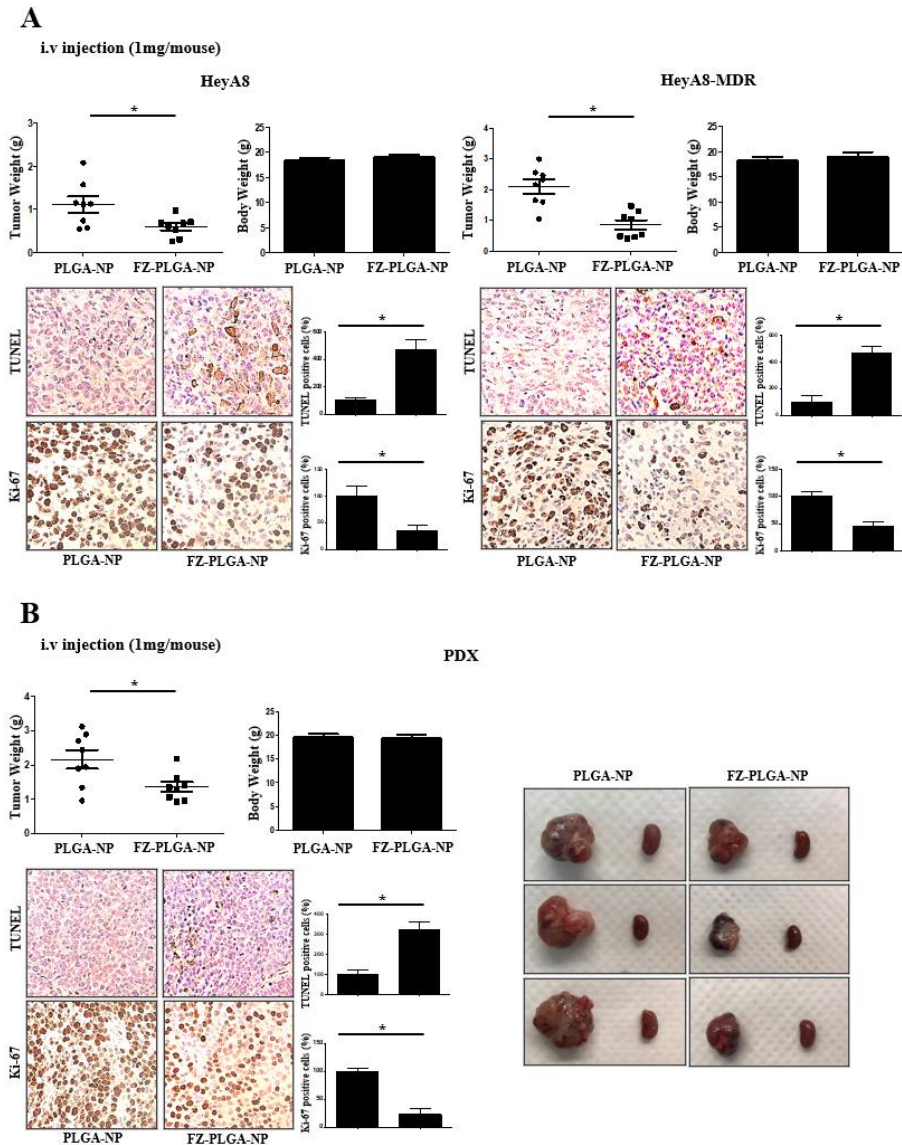


Figure 5. Anti-cancer effect of FZ-PLGA-NPs in vitro and in vivo models. (A) EOC cell-line xenografts models. (B) PDX models ($p < 0.05$). FZ-PLGA-NPs: Fenbendazole-Poly (d,l-lactide-co-glycolide) acid-Nanoparticles; EOC: epithelial ovarian cancer; PDX: Patient-derived xenograft.

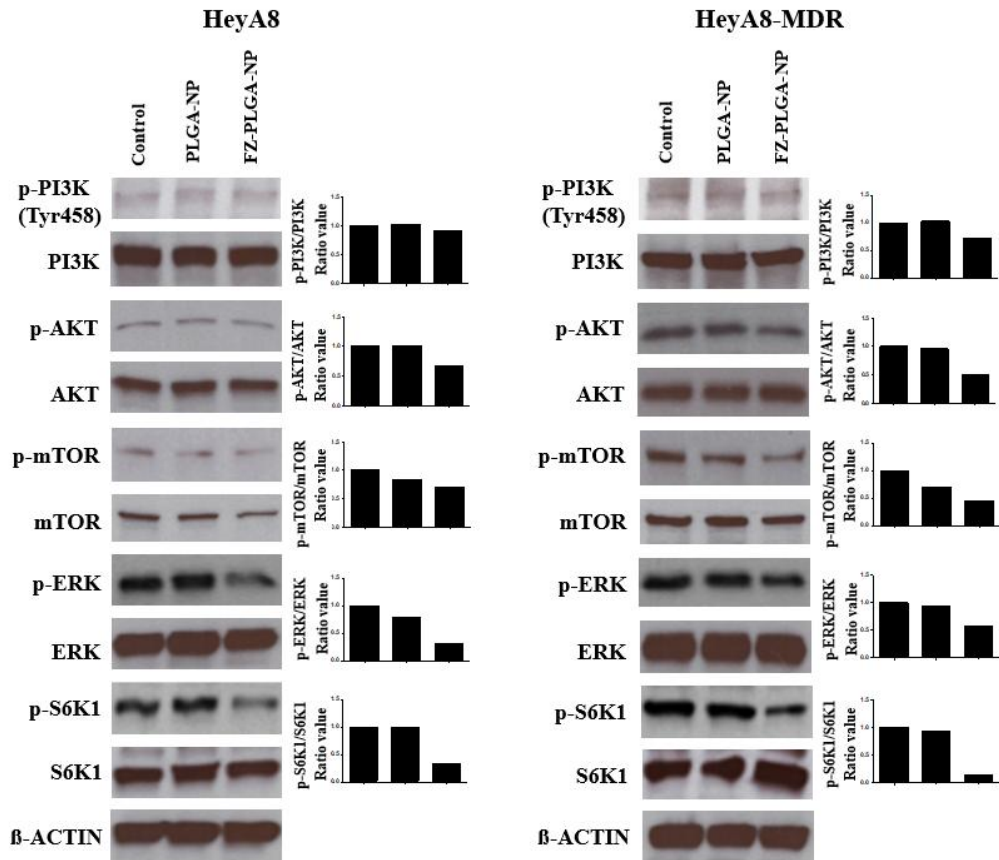


Figure 6. Western blot analysis to evaluate the cell signaling pathway in epithelial ovarian cancer cells.

4. Discussion

In this study, we developed a drug delivery carrier system (FZ-PLGA-NP) to overcome water insolubility of FZ in application for cancer therapy. In addition, FZ-PLGA-NP significantly showed anti-cancer effects in cell proliferation and apoptosis in EOC cells. We also confirmed that FZ-PLGA-NP significantly inhibited tumor growth in cell line xenograft and PDX models.

Benzimidazole anthelmintics, including fenbendazole, have been used since their introduction in 1960s (26). They selectively bind to β -tubulin of parasitic worms, causing their immobilization and death. Due to the selective affinity with microtubules, benzimidazole anthelmintics have been extensively explored as anti-cancer drugs for drug repurposing. They have been shown to inhibit cell viability in a variety of cancer cell lines, including colorectal, liver, lung, and brain tumors (27-30). In addition to the disruption of microtubule polymerization, previous studies have suggested several potential mechanisms of benzimidazole anthelmintics, such as inhibition of cell proliferation and induction of apoptosis, cell cycle arrest, and blockade of glucose transport (12). In ovarian cancer models, the main anti-cancer mechanism proven was anti-angiogenesis of albendazole through down-regulation of VEGF (13-15). This study added more evidence to the anti-cancer mechanism in ovarian cancer models that FZ affects cell proliferation through inhibition of PI3K/AKT and MAPK signaling pathways.

Previous reports in ovarian cancer animal model demonstrated anti-tumor effect of IP administration of albendazole, but the dose of the drug was very high ranging 150 mg/kg to 450 mg/kg (13-15),

whereas acceptable dose for human use of albendazole is up to 400 mg per day (12). Due to its low water solubility and bioavailability, it must have been used at such a high dose to exhibit a cytotoxic effect. However, the dose was too high that it can easily be expected to be highly toxic when clinically applied. Therefore, various methods for increasing solubility of benzimidazole anthelmintics were proposed. Pourgholami et al. (31) and Pillai et al. (32) suggested attaching cyclodextrin, a cyclic oligosaccharide, to improve poor aqueous solubility of albendazole. Nanoparticle drug delivery system was next being presented for improving water solubility. Albumin nanoparticle carrying albendazole was assembled, and demonstrated anti-cancer effect in EOC animal model at a much lower drug dose of 10 mg/kg (33). In other cancer types, several other nanoparticles have been developed to overcome poor aqueous solubility of FZ in prostate cancer and glioma (34,35). We utilized PLGA-NP as a platform to deliver FZ effectively to EOC tumor cells, and successfully demonstrated anti-cancer effect with low toxicity in animal models.

Nanoparticle system is an attractive system that can carry a large payload of drugs compared with antibody conjugates (36). Furthermore, drugs are located within the particle so that their pharmaceutical properties may not affect the distribution of the nanoparticle itself (23). Among various types of nanoparticle system, PLGA-NPs are widely used for targeted delivery of drugs due to their low toxicity and high biocompatibility (37). Several studies have used PLGA-NPs for targeted delivery of cisplatin or paclitaxel for drug-resistant ovarian cancer (38-40). The attachment of targeting ligands which enable particular interactions between the nanoparticle and the target cell surface may be a key role in the delivery of nanoparticle.

In our study, FZ-PLGA-NP showed cytotoxic effect on EOC models using paclitaxel-resistant HeyA8-MDR cell line as well as models with chemosensitive EOC cells. Targeted delivery of FZ-PLGA-NPs with appropriate ligand might enhance anti-cancer effect for chemoresistant EOC, and further research is needed in this regard.

In conclusion, we demonstrated the anti-cancer effect of FZ in various drug delivery modes for EOC models. Natural form of FZ was effective to EOC cells in vitro, but neither oral nor IP administration in vivo had any effect due to water insolubility of the drug. We combined FZ with PLGA-NPs for the first time. Anti-cancer effect to EOC cells was identified both in vitro and in vivo including PDX models in water soluble form of FZ-PLGA-NPs. FZ-PLGA-NPs induced changes of signals in cell proliferation and apoptosis. Further experiments and clinical trials should be considered in the future for clinical use of FZ in ovarian cancer treatment.

5. Summary

EOC is fatal gynecologic malignancy. Although there are standard treatments, most patients experience relapse and eventually die from the disease. Therefore, new drug strategies are needed to overcome EOC. Several studies have demonstrated that benzimidazole drugs have anti-cancer effects.

We investigate the anti-cancer effect of FZ on EOC models including in various drug delivery modes for EOC models. Natural form of FZ was effective to EOC cells in vitro, but neither oral nor IP administration in vivo had any effect due to water insolubility of the drug. Therefore, in order to overcome the hydrophobicity of FZ, we combined FZ with PLGA-NPs.

Anti-cancer effect to EOC cells was identified both in vitro and in vivo including PDX models in water soluble form of FZ-PLGA-NPs. FZ-PLGA-NPs induced changes of signals in cell proliferation and apoptosis.

Further experiments and clinical trials should be considered in the future for clinical use of FZ in ovarian cancer treatment.

References

1. Siegel RL, Miller KD, Fuchs HE, Jemal A: Cancer statistics, 2022. *CA Cancer J Clin* 2022; 72: 7-33.
2. Kuroki L, Guntupalli SR: Treatment of epithelial ovarian cancer, *BMJ* 2020; 371: m3773.
3. Lee JM, Minasian L, Kohn EC: New strategies in ovarian cancer treatment, *Cancer* 2019; 125(Suppl 24): 4623-9.
4. Ozols RF: Treatment goals in ovarian cancer. *Int J Gynecol Cancer* 2005; 15(Suppl 1): 3-11.
5. Yancik R: Ovarian cancer. Age contrasts in incidence, histology, disease stage at diagnosis, and mortality. *Cancer* 1993; 71(2 Suppl): 517-23.
6. Mrkvova Z, Uldrijan S, Pombinho A, Bartunek P, Slaninova I: Benzimidazoles downregulate Mdm2 and MdmX and activate p53 in MdmX overexpressing tumor cells. *Molecules* 2019; 24: 2152.
7. Duan Q, Liu Y, Booth CJ, Rockwell S: Use of fenbendazole-containing therapeutic diets for mice in experimental cancer therapy studies. *J Am Assoc Lab Anim Sci* 2012; 51: 224-30.
8. Duan Q, Liu Y, Rockwell S: Fenbendazole as a potential anticancer drug. *Anticancer Res* 2013; 33: 355-62.

9. Dogra N, Kumar A, Mukhopadhyay T: Fenbendazole acts as a moderate microtubule destabilizing agent and causes cancer cell death by modulating multiple cellular pathways. *Sci Rep* 2018; 8: 11926.
10. Tang Y, Liang J, Wu A, Chen Y, Zhao P, Lin T, et al.: Co-delivery of trichosanthin and albendazole by nano-self-assembly for overcoming tumor multidrug-resistance and metastasis. *ACS Appl Mater Interfaces* 2017; 9: 26648-64.
11. Chu SW, Badar S, Morris DL, Pourgholami MH: Potent inhibition of tubulin polymerization and proliferation of paclitaxel-resistant 1A9PTX22 Human ovarian cancer cells by albendazole. *Anticancer Res* 2009; 29: 3791-6.
12. Son DS, Lee ES, Adunyah SE: The antitumor potentials of benzimidazole antihelminthics as repurposing drugs. *Immune Netw* 2020; 20: e29.
13. Pourgholami MH, Yan Cai Z, Lu Y, Wang L, Morris DL: Albendazole: a Potent Inhibitor of vascular endothelial growth factor and malignant ascites formation in OVCAR-3 tumor-bearing nude mice. *Clin Cancer Res* 2006; 12: 1928-35.
14. Choi EK, Kim SW, Nam EJ, Paek J, Yim GW, Kang MH, et al.: Differential effect of intraperitoneal albendazole and paclitaxel on ascites formation and expression of vascular endothelial growth factor in ovarian cancer cell-bearing athymic nude mice. *Reprod Sci* 2011; 18: 763-71.

15. Pourgholami MH, Cai ZY, Chu SW, Galettis P, Morris DL: The influence of ovarian cancer induced peritoneal carcinomatosis on the pharmacokinetics of albendazole in nude mice. *Anticancer Res* 2010; 30: 423-8.
16. Dayan AD: Albendazole, mebendazole and praziquantel. Review of non-clinical toxicity and pharmacokinetics. *Acta Trop* 2003; 86: 141-59.
17. Juere E, Caillard R, Kleitz F: Pore confinement and surface charge effects in protein-mesoporous silica nanoparticles formulation for oral drug delivery. *Microporous Mesoporous Mater* 2020; 306: 110482. Available from: URL:<https://www.sciencedirect.com/science/article/pii/S1387181120304844>
18. Livney YD, Assaraf YG: Rationally designed nanovehicles to overcome cancer chemoresistance. *Adv Drug Deliv Rev* 2013; 65: 1716-30.
19. Xu X, Xie K, Zhang XQ, Pridgen EM, Park GY, Cui DS, et al.: Enhancing tumor cell response to chemotherapy through nanoparticle-mediated codelivery of siRNA and cisplatin prodrug. *Proc Natl Acad Sci U S A* 2013; 110: 18638-43.
20. Ye H, Karim AA, Loh XJ: Current treatment options and drug delivery systems as potential therapeutic agents for ovarian cancer: a review. *Mater Sci Eng C Mater Biol App* 2014; 45: 609-19.
21. Kapoor DN, Bhatia A, Kaur R, Sharma R, Kaur G, Dhawan S: PLGA: a

- unique polymer for drug delivery. *Ther Deliv* 2015; 6(1): 41-58.
22. Hickey T, Kreutzer D, Burgess DJ, Moussy F: Dexamethasone/PLGA microspheres for continuous delivery of an anti-inflammatory drug for implantable medical devices. *Biomaterials* 2002; 23(7): 1649-56.
23. Byeon Y, Lee JW, Choi WS, Won JE, Kim GH, Kim MG, et al.: CD44-Targeting PLGA Nanoparticles Incorporating Paclitaxel and FAK siRNA Overcome Chemoresistance in Epithelial Ovarian Cancer. *Cancer Res* 2018; 78(21): 6247-56.
24. Saad AS, Attia AK, Alaraki MS, Elzanfaly ES: Comparative study on the selectivity of various spectrophotometric techniques for the determination of binary mixture of fenbendazole and rafoxanide. *Spectrochim Acta A Mol Biomol Spectrosc* 2015; 150: 682-90.
25. de Silva N, Guyatt H, Bundy D: Anthelmintics. A comparative review of their clinical pharmacology. *Drugs* 1997; 53: 769-88.
26. Furtado LFV, de Paiva Bello ACP, Rabelo EML: Benzimidazole resistance in helminths: from problem to diagnosis. *Acta Trop* 2016; 162: 95-102.
27. Michaelis M, Agha B, Rothweiler F, Loschmann N, Voges Y, Mittelbronn M, et al.: Identification of flubendazole as potential anti-neuroblastoma compound in a large cell line screen. *Sci Rep* 2015; 5: 8202.
28. Sasaki J, Ramesh R, Chada S, Gomyo Y, Roth JA, Mukhopadhyay T:

- The anthelmintic drug mebendazole induces mitotic arrest and apoptosis by depolymerizing tubulin in non-small cell lung cancer cells. *Mol Cancer Ther* 2002; 1: 1201-9.
29. Mukhopadhyay T, Sasaki J, Ramesh R, Roth JA: Mebendazole elicits a potent antitumor effect on human cancer cell lines both in vitro and in vivo. *Clin Cancer Res* 2002; 8: 2963-9.
30. Lin S, Yang L, Yao Y, Xu L, Xiang Y, Zhao H, et al.: Flubendazole demonstrates valid antitumor effects by inhibiting STAT3 and activating autophagy. *J Exp Clin Cancer Res* 2019; 38: 293.
31. Pourgholami MH, Wangoo KT, Morris DL: Albendazole-cyclodextrin complex: enhanced cytotoxicity in ovarian cancer cells. *Anticancer Res* 2008; 28: 2775-9.
32. Pillai K, Akhter J, Morris DL: Super aqueous solubility of albendazole in β -cyclodextrin for parenteral application in cancer therapy. *J Cancer* 2017; 8: 913-23.
33. Noorani L, Stenzel M, Liang R, Pourgholami MH, Morris DL: Albumin nanoparticles increase the anticancer efficacy of albendazole in ovarian cancer xenograft model. *J Nanobiotechnology* 2015; 13: 25.
34. Marslin G, Siram K, Liu X, Khandelwal VKM, Xiaolei S, Xiang W, et al.: Solid lipid nanoparticles of albendazole for enhancing cellular uptake and cytotoxicity against U-87 MG glioma cell lines. *Molecules* 2017; 22: 2040.

35. Esfahani MKM, Alavi SE, Cabot PJ, Islam N, Izake EL: β -Lactoglobulin-Modified Mesoporous Silica Nanoparticles: A Promising Carrier for the Targeted Delivery of Fenbendazole into Prostate Cancer Cells. *Pharmaceutics* 2022; 14: 884.
36. Kirtane AR, Kalscheuer SM, Panyam J: Exploiting nanotechnology to overcome tumor drug resistance: challenges and opportunities. *Adv Drug Deliv Rev* 2013; 65: 1731-47.
37. Acharya S, Sahoo SK: PLGA nanoparticles containing various anticancer agents and tumour delivery by EPR effect. *Adv Drug Deliv Rev* 2011; 63: 170-83.
38. Zhu X, Yan S, Xiao F, Xue M: PLGA nanoparticles delivering CPT-11 combined with focused ultrasound inhibit platinum resistant ovarian cancer. *Transl Cancer Res* 2021; 10: 1732-43.
39. Dominguez-Rios R, Sanchez-Ramirez DR, Ruiz-Saray K, Ocegüera-Basurto PE, Almada M, Juárez J, et al.: Cisplatin-loaded PLGA nanoparticles for HER2 targeted ovarian cancer therapy. *Colloids Surf B Biointerfaces* 2019; 178: 199-207.
40. Wang Y, Qiao X, Yang X, Yuan M, Xian S, Zhang L, et al.: The role of a drug-loaded poly (lactic co-glycolic acid) (PLGA) copolymer stent in the treatment of ovarian cancer. *Cancer Biol Med* 2020; 17: 237-50.

Anti-cancer Effect of Fenbendazole Incorporated PLGA Nanoparticles in Ovarian Cancer

Choi, June Kuk

Department of Obstetrics & Gynecology
Graduate School

Keimyung University

(Supervised by Professor Kwon, Sang Hoon)

(Abstract)

Epithelial ovarian cancer (EOC) has a poor prognosis, and there is an unmet need to find new therapeutic drugs. Fenbendazole (FZ) is an anti-helminthic drug acting as microtubule-disrupting agent, and previous studies suggested this drug to have anticancer effects. Because of the reduced drug efficacy due to the hydrophobicity of FZ, in this study, we combined FZ with poly (lactic-co-glycolic acid) (PLGA) nanoparticles to obtain hydrophilicity. We further investigated the anticancer effect of FZ with different drug delivery method on EOC cells in both in vitro and in vivo. Anti-cancer effect to EOC cells was identified both in vitro and in vivo including PDX models in water soluble form of FZ-PLGA-NPs. FZ-PLGA-NPs induced changes of signals in cell proliferation and apoptosis.

난소암에 펜벤다졸이 포함된 PLGA 나노 입자의 항암 효과

최 준 국
계명대학교 대학원
의학과 산부인과학 전공
(지도교수 권 상 훈)

(초록)

상피성 난소암은 예후가 좋지 않으며, 새로운 치료제에 대한 개발이 요구된다. 펜벤다졸은 미세소관 교란제로 작용하는 구충제이며 이전의 연구에서 이 약물이 항암 효과가 있다고 밝혀져있다. 펜벤다졸의 소수성으로 인한 약물 효과 저하 때문에 이 연구에서는 친수성을 얻기 위해 펜벤다졸과 폴리(락트산-코-글리콜산)(PLGA) 나노입자를 결합하였다. 우리는 시험관 내 및 생체 내에서 상피성 난소암 세포주에 대한 다른 약물 전달 방법에 따른 펜벤다졸의 항암 효과를 추가로 조사하였다. 상피성 난소암 세포주에 대한 항암 효과는 펜벤다졸-PLGA-나노입자의 수용성 형태의 환자 유래 이중이식 모델을 포함하여 시험관 내 및 생체 내 모두에서 확인되었다. 펜벤다졸-PLGA-나노입자는 세포 증식과 세포 사멸에서 효과를 보였다.